IEEE Access
Multidisciplinary | Rapid Review | Open Access Journal

Received 1 July 2023, accepted 29 July 2023, date of publication 2 August 2023, date of current version 11 August 2023.

Digital Object Identifier 10.1109/ACCESS.2023.3301125

RESEARCH ARTICLE

Research on the Nonlinear Dynamic Behavior of H-Bridge Inverter Based on Joint PI and Improved Power Reaching Law Sliding Mode Control

WEI JIANG[1], MING JIAN WU[1], AND FANG YUAN[2]
[1]Department of Intelligent Manufacturing, Wuyi University, Jiangmen 529000, China
[2]School of Mechanical and Electronic Engineering, East China University of Technology, Nanchang 330039, China

Corresponding author: Ming Jian Wu (240114298@qq.com)

This work was supported in part by the Science and Technology Plan Project of the Education Department of Jiangxi Province under Grant GJJ2203702; in part by the Jiangmen Science and Technology Plan Project under Grant 202187; and in part by the Innovative Entrepreneurship Plan for College Students under Grant 202111349125, Grant 20211134919, Grant S202211349130X, and Grant 202211349156.

ABSTRACT To broaden the stability domain of the H-bridge inverter, a control method of the H-bridge inverter combined with PI and improved power reaching law sliding mode control is studied in this paper. To analyze the complex dynamical behavior of this inverter, firstly, the mathematical model of this system is established and numerical simulation of this model is performed. Secondly, the nonlinear dynamical behavior of this inverter is observed by a bifurcation diagram, folding diagram, stroboscopic diagram, time-domain diagram, and spectral diagram. Thirdly, the stability theory of the system is analyzed by applying the fast-varying stability theorem, and the consistency between the theoretical analysis and numerical simulation further proves the mechanism of nonlinear dynamical behavior occurring in this inverter. Finally, the influence of the circuit parameters: input voltage, load inductance, and load resistance on the nonlinear dynamical behavior of the inverter is analyzed. It is shown that this joint control mode can broaden the operating stability domain of the H-bridge inverter, which provides an important theoretical basis for the design and manufacture of the inverter.

INDEX TERMS H-bridge inverter, nonlinear, chaos, bifurcation, discrete mode.

I. INTRODUCTION

H-bridge inverter system is a typical nonlinear system, which shows strong complex dynamic characteristics, which has an important impact on the stability and reliability of the system. When the circuit parameters are not designed properly, electromagnetic noise, intermittent oscillation, and even sudden collapse will occur in the use of the system, resulting in severe challenges to the working stability of the system. In response to the complex dynamical behavior that occurs in the H-bridge inverter system, many experts and scholars have studied the nonlinear dynamical behavior of the H-bridge inverter in recent years [1], [2], [3], [4].

In [5], the chaos and bifurcation of the H-bridge converter with reference current as DC and current control mode are studied for the first time. The inverter's nonlinear behavior due to changes in circuit parameters (such as k, R, and L) is analyzed using bifurcation diagrams. The results are of great significance for designing and debugging single-phase H-bridge inverters [6]. In the study of the parallel single-phase H-bridge inverter, two scales, fast and slow variation, were introduced and both types of instabilities were discussed from a practical design point of view, and these findings can be used to guide the adjustment of the inverter system parameters [7]. The stability of a PI-controlled current-controlled H-bridge passive inverter is thoroughly analyzed, including establishing a discrete iterative mapping model, analyzing dynamic bifurcation behavior, and exploring the influence of other parameters on system stability. This analysis

The associate editor coordinating the review of this manuscript and approving it for publication was Ludovico Minati.

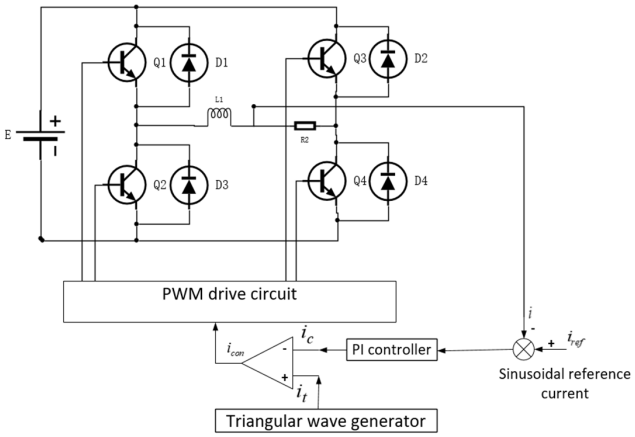

FIGURE 1. Working principle diagram of H-bridge inverter based on PI control.

provides valuable reference for designing and applying H-bridge inverters [8]. To solve the jitter problem of sliding mode control, an chattering free improved sliding mode control is proposed to improve the stability and anti-interference of the system [9]. A fast-varying stability theorem for H-bridge inverters with sliding-mode control is proposed, which can be used to analyze whether the system is in a stable state or not [10]. A new algorithm based on the combination of sliding-mode variable structure control and fractional-order PID control is studied and proposed. Experimental results show that the algorithm has excellent control performance with fast convergence, small error, and robustness [11]. Experiments show that the algorithm has fast convergence, small errors, strong robustness, and excellent control performance. In recent years, these studies provide an important theoretical basis for the design of the inverter, and it is of great practical significance to control the nonlinear dynamic behavior.

To broaden the stability domain of the system, this paper studies a control mode based on the combination of linear control and nonlinear control, which is based on the H-bridge inverter under the combined control of PI and improved power reaching law sliding mode. The discrete mathematical model under the control mode is established, and the nonlinear dynamic behavior of the system is observed by bifurcation, folding, stroboscopic and time-domain diagrams, and by frequency spectrum and other methods, and the fast-varying stability theorem is used for in-depth theoretical analysis. he influence of external circuit parameters on the nonlinear dynamic behavior of the system is studied, the stable working range of the H-bridge inverter is broadened, and a reliable theoretical basis is provided for the design of the inverter.

II. SYSTEM MODEL OF H-BRIDGE INVERTER BASED ON PI AND IMPROVED POWER REACHING LAW

A. MODELING OF H-BRIDGE INVERTER CONTROLLED BY PI

Based on the H-bridge inverter controlled by PI, the circuit has two working states in a switching cycle. The modulated signal i_c is compared with the triangular wave i_t. State 1: when i_c is greater than i_t, PWM high-level output, D_1 and D_4 are turned on, D_2 and D_3 are off; state 2: when i_c is less than i_t, PWM low-level output, D_1 and D_4 are off, D_2 and D_3 are turned on, as shown in Figure 1.

d_n is the duty cycle of state 1, and its expression is given in formula (1)

$$d_{\mathrm{n}} = \begin{cases} 0, & (d_{\mathrm{n}} \le 0) \\ \dfrac{1}{2}(1 + \dfrac{i_c}{I_H}) & (0 < d_{\mathrm{n}} < 1) \\ 1, & (d_{\mathrm{n}} \ge 1) \end{cases} \tag{1}$$

The inverter switches repeatedly between states 1 and 2, and the state equation of the main circuit in the nth switching cycle T_{s} is given by formulas (2) and (3):

$$\frac{di}{dt} = -\frac{R}{L}\mathrm{i} + \frac{E}{L}, \quad nT_{\mathrm{S}} < \mathrm{t} \le (n + \mathrm{d_n})nT_{\mathrm{s}} \tag{2}$$

$$\frac{di}{dt} = -\frac{R}{L}\mathrm{i} - \frac{E}{L}, \quad (n + d_n)T_{\mathrm{s}} < t \le (n + 1)T_s \tag{3}$$

According to the stroboscopic mapping theory [12], [13], [14], the switching period T_{s} is taken as the time interval of stroboscopic sampling, and the sampling value of the state variable in the nth switching period is used to represent the sampling value of the state variable in the nth plus 1 switching period. The discrete iterative model of the inverter main circuit is derived (4):

$$i_{n+1} = e^{-\frac{R}{L}T_s} i_n + [\frac{2}{R} e^{-\frac{(1-d_n)RT_s)}{L}} - \frac{1}{R}(1 + e^{-\frac{R}{L}T_s})]E \tag{4}$$

i_{n} is the value of inductor current at sampling time. The state equation of modulated signal can be obtained by inverse Laplace transform (5):

$$\frac{di_c}{dt} = -k_p \frac{di_e}{dt} - k_i i_e + u \tag{5}$$

In the above formula: $i_e = i_{ref} - i$,

$$u = k_p \frac{di_{ref}}{dt} + k_i i_{ref}, \quad i_{ref} = i_{ref\,\max} \sin \omega n T_s, \ \omega = 2\pi f,$$

k_{p}, k_{i} are proportional and integral parameters, respectively.

The modulation circuit is analyzed in the frequency domain, from the transfer function G(s) of the PI controller and Figure 1:

$$G_c(s) = k_p + \frac{k_i}{s} \tag{6}$$

$$i_c(s) = G_c(s) i_e(s) \tag{7}$$

$i_c(s)$ and $i_e(s)$ are the input and output variables of the PI controller, respectively, which are obtained from equations (6) and (7):

$$s i_c(s) = k_p s i_e(s) + k_i i_e(s) \tag{8}$$

The time domain equation of equation (8) is obtained after Laplace transform:

$$\frac{di_c(t)}{dt} = k_p \frac{di_e(t)}{dt} + k_i i_e(t) \tag{9}$$

After substituting i_e into equation (9), equation (10) is obtained:

$$\frac{di_c(t)}{dt} = -k_p\frac{di_e(t)}{dt} - k_i i(t) + k_p\frac{di_{ref}(t)}{dt} + k_i i_{ref}(t) \quad (10)$$

When $nT_S < t \le (n + d_n)nT_s$, equation (11) can be obtained from equation (2).

$$i(t) = -\frac{L}{R}\frac{di(t)}{dt} + \frac{E}{R} \quad (11)$$

Substituting equation (11) into equation (10), we can obtain equation (12):

$$\frac{di_c(t)}{dt} = (k_i\frac{L}{R} - k_p)\frac{di(t)}{dt} - k_i\frac{E}{R} + u(t) \quad (12)$$

In equation (12), the

$$u(t) = k_p\frac{di_{ref}(t)}{dt} + k_i i_{ref}(t) \quad (13)$$

The equation of state of the modulation circuit is shown in equation (12), and the iterative model is derived from the stroboscopic mapping theory. The reference current is set as a sine wave, and the sampling gap is taken as the clock period T_s, for which the discrete derivation, since $f \ll f_s$, within the nth clock period T_s, i_{ref} can be considered as a constant value, $i_{refn} = A\sin(\omega nT_s)$, so u(t) can be expressed as follows:

$$U_n = k_i A\sin(\omega nT_s) \quad (14)$$

When $nT_S < t \le (n + d_n)nT_s$, the inverter works in state 1, and the load current value of the main circuit at $(n + d_n)\ T_s$ can be deduced from equation (2):

$$i_{n+d_n} = (in - \frac{E}{R})e^{\frac{d_n T_s R}{L}} + \frac{E}{R} \quad (15)$$

According to equation (15), discrete treatment of equation (12) leads to equation (16):

$$i_c(n + d_n) = (k_i\frac{L}{R} - k_p)i_c(n + d_n) - (k_i\frac{L}{R} - k_p)i_n + (-k_i\frac{E}{R} + U_n)d_nT_s + i_c(n) \quad (16)$$

When $(n+d_n)T_s < t \le (n+1)T_s$, equation (12) then becomes equation (17):

$$\frac{di_c(t)}{dt} = (k_i\frac{L}{R} - k_p)\frac{di(t)}{dt} + k_i\frac{E}{R} + u(t) \quad (17)$$

According to equation (16), discrete treatment of equation (17) leads to equation (18):

$$i_c(n + 1) = (k_i\frac{L}{R} - k_p)(i_{n+1} - i_n) + i_c(n) + k_i\frac{E}{R}T_s(1 - 2d_n) + T_sU_n \quad (18)$$

The discrete iterative model of the circuit is obtained by substituting equation (4) into equation (18). The discrete model of H-bridge inverter controlled by PI is formula(19):

$$i_c(n) = a_1 i_{n-1} + i_c(n - 1) + a_2E + T_sU_{n-1} \quad (19)$$

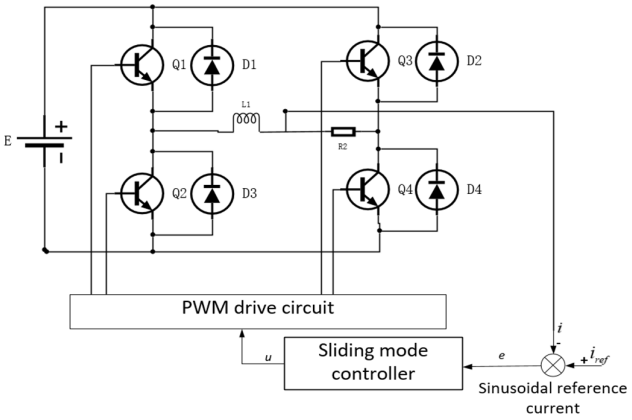

FIGURE 2. Working principle diagram of H-bridge inverter with sliding mode control.

In formula(19):

$$a_1 = (\frac{L}{R}k_i - k_p)(e^{-\frac{R}{L}T_s} - 1) \quad (20)$$

$$a_2 = (\frac{L}{R}k_i - k_p)(\frac{2}{R}e^{-\frac{R(1-d_n)}{L}T_s} - \frac{1}{R} - \frac{1}{R}e^{-\frac{R}{L}T_s}) + a_3 \quad (21)$$

$$a_3 = \frac{k_iT_s}{R}(1 - 2d_{n-1}) \quad (22)$$

$$U_{n-1} = k_p i_{ref\ \max}\omega\cos\omega(n - 1)T_s + a_4 \quad (23)$$

$$a_4 = k_i i_{ref\ \max}\sin\omega(n - 1)T_s \quad (24)$$

B. MODELING OF H-BRIDGE INVERTER BASED ON IMPROVED POWER REACHING LAW SLIDING MODE CONTROL

The circuit consists of a switch tube ($D_1 \sim D_4$), a DC voltage source, a load resistance and an inductor.

The result of the comparison between the load current and the sinusoidal reference current is sent to the sliding mode controller, and the output control variables enter the PWM drive circuit to control the switch on and off. The working: schematic diagram is shown in Figure 2.

According to the principle of sliding mode control, the expression of the control variable is (12)

$$u = -\text{sgn}(e) \quad (25)$$

In the formula: $e = i - i_{ref}$. Because the sliding mode control is easy to produce system chattering, the control system is unstable. The improved power reaching law sliding mode control method is more stable [15], [16], [17], the sliding mode motion quality is better, and the convergence speed is faster. After adding the improved power reaching law, the control variable is expressed as formula (26):

$$u = -k_1\ |e|^a\ \text{sgn}(e) - k_2(e)^2\text{sgn}(e), \quad k_1 > 0, \quad k_2 > 0,\ 0 < a < 1 \quad (26)$$

The nonlinear dynamic behavior of the system is studied, and the discrete model of the system is established according to

the stroboscopic mapping method. The iterative equation is formula(27):

$$i_{n+1} = (i_n - a)e^{-\frac{T_s}{t}} + 2ae^{\frac{-(1-d_n)T_s}{t}} - a \tag{27}$$

d_n represents the duty cycle of the nth switching cycle. According to the boundedness theorem of duty cycle, the following results are obtained:

$$d_{\mathrm{n}} = \begin{cases} 0, & (d_{\mathrm{n}} \le 0) \\ u, & (0 < d_{\mathrm{n}} < 1) \\ 1, & (d_{\mathrm{n}} \ge 1) \end{cases} \tag{28}$$

In the formula(29):

$$u = -k_1 |e|^a \operatorname{sgn}(e) - k_2(e)^2 \operatorname{sgn}(e), \quad k_1 > 0, \quad k_2 > 0, \ 0 < a < 1 \tag{29}$$

e is the difference between the load current sampling value and the reference current sampling value at the nth switching cycle, $e = i_n - i_{ref,n}$, $i_{ref,n} = A\sin(2\pi fnT_s)$. The discrete model of H-bridge inverter with improved power reaching law sliding mode control is composed of formula(25)-(29).

C. MODELING OF H-BRIDGE INVERTER BASED ON JOINT PI AND IMPROVED POWER REACHING LAW SLIDING MODE CONTROL

The joint control mode process involves comparing the load current and reference current, inputting the result of their subtraction to both a PI regulator and a modified power reach method sliding mode controller. The modulating signal is then obtained through joint control, compared with the delta wave, and finally output as a PWM drive signal that turns the switch on or off. The working principle diagram of the system is shown in Figure 3.

d_{n} represents the duty cycle of the nth switching cycle, and the duty cycle of the H-bridge inverter in this control mode is expressed as formula (30):

$$d_{\mathrm{n}} = \begin{cases} 0, & (d_{\mathrm{n}} \le 0) \\ \frac{1}{2}(1 + i_{con}), & (0 < d_{\mathrm{n}} \le 1) \\ 1, & (d_{\mathrm{n}} > 1) \end{cases} \tag{30}$$

$i_{en} = a_1 i_{n-1} + i_{en-1} + a_2 E + T_s U_{n-1}$ can be known from equation (19), From equation (29), we can know that

$$u = -k_1 |e|^a \operatorname{sgn}(e) - k_2(e)^2 \operatorname{sgn}(e), \quad k_1 > 0, k_2 > 0, 0 < a < 1, \tag{31}$$

and $i_{con} = i_c(n) + u$. That is, i_{con} is expressed as an equation (32):

$$i_{con} = a_1 i_{n-1} + i_c(n-1) + a_2 E + T_s U_{n-1} - k_1 |e|^a \operatorname{sgn}(e) - k_2(e)^2 \operatorname{sgn}(e) k_1 > 0, \ k_2 > 0, \ 0 < a < 1. \tag{32}$$

The discrete model of H-bridge inverter under the joint PI and improved power reaching law sliding mode control is composed of formulas (30) and (32).

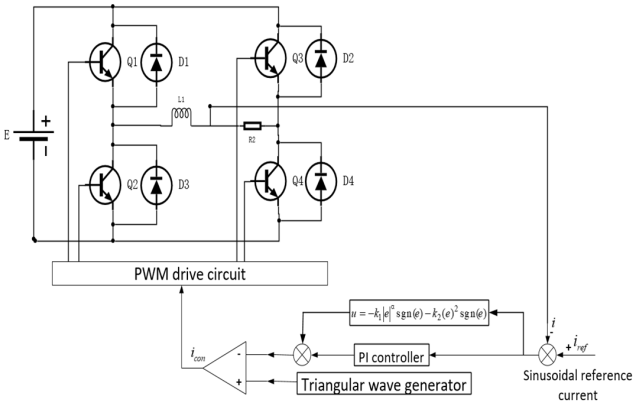

FIGURE 3. Working principle diagram of H-bridge inverter using joint PI and improved power reaching law sliding mode control.

III. ANALYSIS OF NONLINEAR DYNAMIC BEHAVIOR OF H-BRIDGE INVERTER UNDER JOINT PI AND IMPROVED POWER REACHING LAW SLIDING MODE CONTROL

The circuit parameters are set as follows: $k_i = 180$, E = 160V, R = 10Ω, L = 3 mH, f_s = 30kHz, $i_{ref} = 5\sin(40\pi t)$, $k_1 = 0.2$, $k_2 = 0.1$. The nonlinear dynamic behavior of the system under different proportional adjustment parameters - k_p is analyzed by means of a bifurcation diagram, folding diagram, frequency spectrum, and so on [18].

A. COMPARISON OF BIFURCATION DIAGRAMS UNDER JOINT CONTROL MODE OF PI AND IMPROVED POWER REACHING LAW SLIDING MODE

Bifurcation diagram method [19]: The discrete model of the system is utilized to select an iterative initial value randomly, and after achieving stability through iteration, state variables at several fixed switching moments are selected under different bifurcation parameters to construct a graph. The bifurcation diagram of the system is thus derived. If a bifurcation parameter corresponds to one state variable, the system is stable; if a bifurcation parameter has n state variables corresponding to it, the system is still stable and in the n-cycle state; if a bifurcation parameter has an infinite number of state variables corresponding to it, the system is unstable and in the chaotic state.

Through the observation of the bifurcation diagram, the relationship between a parameter in the system and the state variables of the system can be obtained. Using the proportional adjustment parameter - k_{p} as the bifurcation parameter, the bifurcation diagrams of the peak and valley values of the output current varying with k_{p} under two different control modes are drawn when k_{p} is used as the bifurcation parameter.

The peak bifurcation diagram of the load current varying with the proportional adjustment parameter - k_{p} is shown in Figure 4. The peak sampling bifurcation diagram in PI control mode is shown in Figure 4(a). When $k_p > 1.08$, the system enters the multiply-periodic bifurcation state, and the stability domain of k_p is [0.18,1.08] as shown by the bifurcation diagram. The peak sampling bifurcation diagram

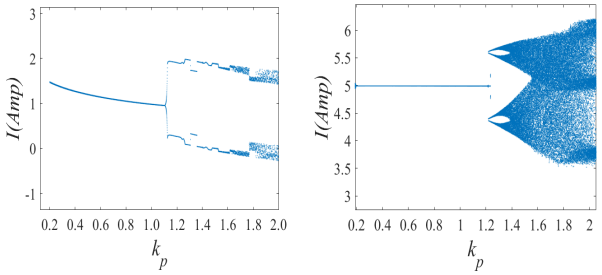

(a) PI control mode (b) joint PI and improved power reaching law sliding mode control

FIGURE 4. Peak bifurcation diagram of load current varying with k_p.

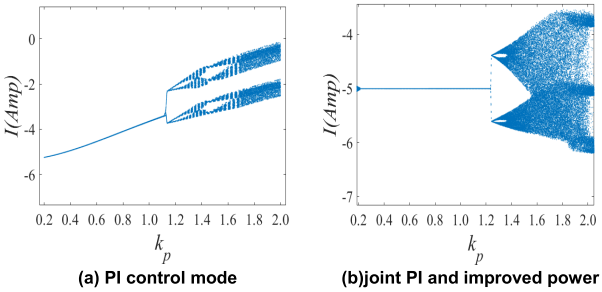

(a) PI control mode (b)joint PI and improved power reaching law sliding mode control

FIGURE 5. Valley bifurcation diagram of load current varying with k_p.

in the joint PI and improved power reaching law sliding mode control is shown in Figure 4(b). For the $k_p = 1.26$ of the stable boundary point in this control mode, it can be seen from the bifurcation diagram that when $0.1 < k_p < 2.0$, the system goes through the process that with the increase of k_p, from the stable state to the period-doubling bifurcation state, and finally to the unstable chaotic state, the parameter range of the stable operation of the system is [0.18, 1.26].

Comparing the bifurcation plots of the two peak samples shows that the inverter has a wider stabilization range with the combination of PI and the improved power convergence law sliding mode control. In the steady state, the peak current in the combined control mode is closer to the reference current peak (5A) as shown in Figure 4(a) and (b).

The valley bifurcation diagram of the load current varies with the proportional adjustment parameter - k_p, as shown in Figure 5. The peak sampling bifurcation diagram in PI control mode is shown in Figure 5(a). When the bifurcation occurs, the critical point is 1.08A, and the valley current is -5.8A. It can be seen from the figure that with the increase of k_p, the system quickly enters a chaotic state; the peak sampling bifurcation diagram under the joint control mode is shown in Figure 5(b). For the $k_p = 1.26$ of the stable demarcation point, the stable region of the system proportional adjustment parameters of the joint control mode is [0.19, 1.26], and the current trough is -5A in the steady state. When $k_p > 1.26$, the system changes from a stable state to a period-doubling bifurcation state and finally enters an unstable chaotic state.

By comparing the bifurcation diagrams sampled at the two valleys, it can be seen that the stable demarcation point of the k_p value of the joint control mode is larger, the stable region is wider, and the current trough in the stable state is closer to the reference current trough.

B. FOLDING DIAGRAM AND TIME-DOMAIN DIAGRAM UNDER THE JOINT CONTROL MODE

The initial value of any iteration is substituted into the discrete equation of the system for iteration, several periods after stability are selected, and several periods are aligned according to the sampling time, and then folded, a system folding diagram can be obtained. the folding diagram can directly reflect the nonlinear dynamic behavior of the system. The folding diagram shows one curve for stable motion; two curves for divergent motion; and irregular points for chaotic motion.

When the integral adjustment factor k_i is 180 and the proportional adjustment factor - k_p is 0.45, 1.35, 1.8 respectively, the folding diagram and time-domain diagram of the system is drawn, as shown in Figure 6. It can be seen from Figure 6(a) that when $k_p = 0.45$ the folded graph is a smooth sinusoidal curve, the inverter is in a stable period 1 state, and the time-domain diagram is also in a period 1 state; when $k_p = 1.35$, the folded graph is two smooth sinusoidal curves, the system works in a period-doubling bifurcation state, and the time-domain diagram also shows a period 2 state. When $k_p = 1.8$, the display area of the folding graph is densely filled with sampling points, indicating that the inverter enters a chaotic state and the time-domain map also works in a chaotic state.

The research shows that when k_i is selected, the conclusions of the bifurcation diagram, folding diagram and time-domain diagram of the system varying with k_p are consistent.

C. STROBE DIAGRAM AND SPECTRUM DIAGRAM UNDER JOINT CONTROL MODE

The nonlinear dynamic behavior of the system under different proportional parameters is further observed by a stroboscopic diagram and spectrum analysis. The specific implementation steps of the stroboscopic sampling map are as follows: according to the discrete model of the system, sampling is carried out at a certain time interval in the process of iterative stability, and the value of the sampling points is maintained [20].

When the integral adjustment factor $k_i = 180$, select k_p equal to 0.45, 1.35, 1.8 respectively, and draw the strobe diagram and spectrum diagram of the system, as shown in Figure 7. The intensity of the spectrum represents the distribution shape of the amplitude of the signal in the spectrum. The stroboscopic diagram and spectrum diagram are used for numerical analysis to further verify the stable region of the proportional parameter k_p of the H-bridge inverter under the joint control mode.

As can be seen from Figure 7 (a), when the $k_p = 0.45$ and the strobe diagram is a smooth sinusoidal curve, the spectrum

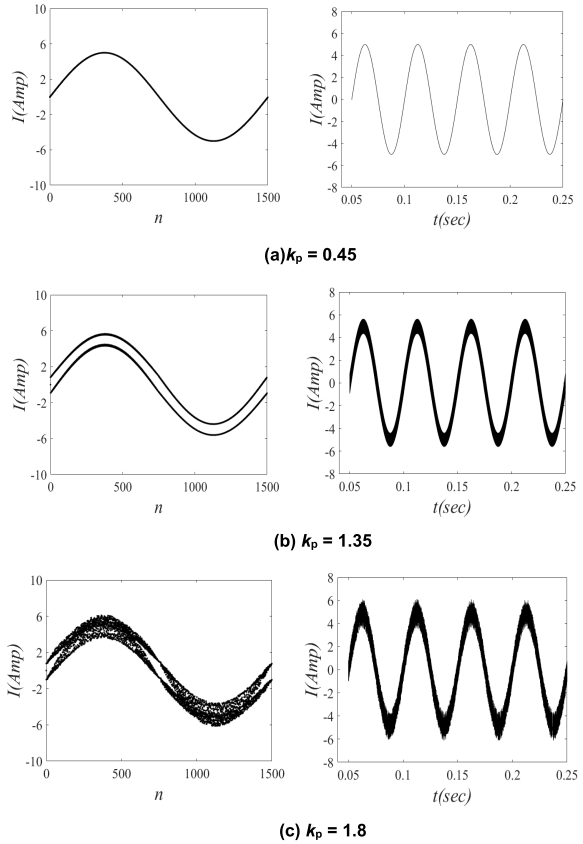

FIGURE 6. Folding diagram (left) and time-domain diagram (right) under different k_p values at $k_i = 180$.

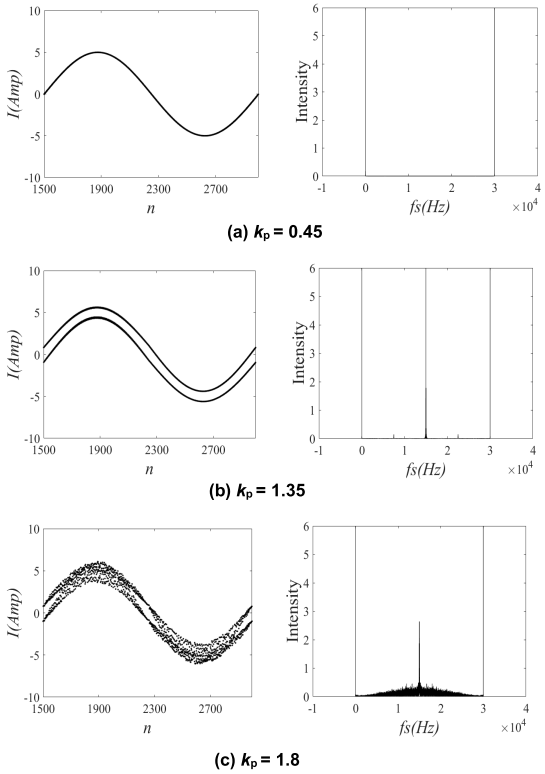

FIGURE 7. Stroboscopic diagram (left) and spectral diagram (right) under different k_p values at $k_i = 180$.

diagram shows only the fundamental frequency, and the inverter operates in a stable period 1 state; when $k_p = 1.35$, the strobe diagram shows two smooth curves near the peak and trough, indicating that the system is period-doubling, and the spectrum diagram shows a bisector shape. When $k_p = 1.8$, the sampling points are densely distributed near the peak and valley values of the strobe map, the system enters a chaotic state, and the spectrum is continuous.

The research shows that when k_i is selected, the bifurcation diagram, strobe diagram, and spectral diagram of the system change with k_p are consistent.

IV. STABILITY ANALYSIS OF SYSTEM BASED ON FAST VARIATION STABILITY THEOREM

Lyapunov index method, Jacobian matrix method, bifurcation diagram, and folding diagram are common methods to analyze the stability of inverter. In the theoretical analysis of stability, both the Lyapunov index method and the Jacobian matrix method need to solve the iterative equation of the system by derivative. However, there is a non-differentiable part of the discrete equation of the H-bridge inverter system under the joint joint control mode, so the above two analysis methods can not be used.

In order to further verify the consistency between the results of simulation analysis and theoretical analysis, such as the bifurcation diagram, folding diagram, and spectrum diagram, the fast-varying stability theorem method is used to analyze the stability of the H-bridge inverter with a joint control mode. the core idea is to take the M switching period near the zero point of the current drop section. The duty cycle of each switching cycle and the duty cycle of the next switch cycle are compared as the difference and divided by the absolute value of the difference, and the number of calculated M is added to get the P value [10]. The expression of P is as follows(33):

$$P = \sum_{n=N_0}^{N_0+M} \frac{d_n - d_{n+1}}{|d_n - d_{n+1}|} \tag{33}$$

In the formula, d_n is the duty cycle in the nth switching cycle, and d_{n+1} is the duty cycle in the n+1 switching cycle. The absolute value of the difference is divided by the difference between the duty cycle of each switching cycle and the duty cycle of the next switching cycle, and the calculated M numbers are added together to obtain P. The current drop is obtained by taking M switching cycles near the zero point. When the system is in a stable state, P = M. When the system is unstable, P < M. After substituting the duty cycle expression (30) in the formula (33), the calculation formula for the stability analysis of the H-bridge inverter with the joint control mode can be obtained.

$$P = \sum_{n=N_0}^{N_0+M} \frac{i_{con}(n) - i_{con}(n+1)}{|i_{con}(n) - i_{con}(n+1)|} \tag{34}$$

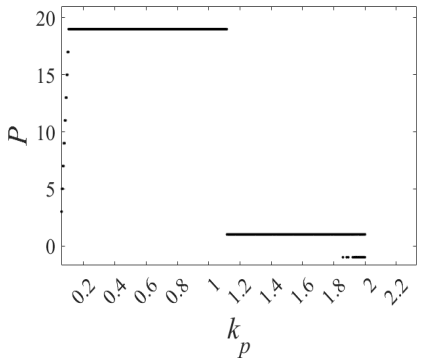

(a) PI control mode

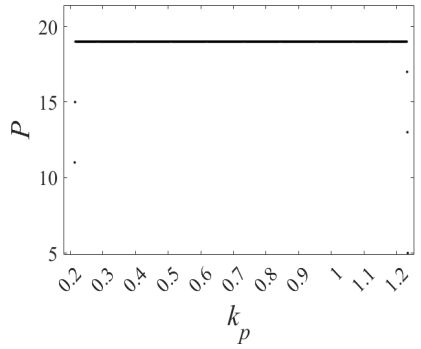

(b) joint PI and improved power reaching law sliding mode control

FIGURE 8. Judgment result of fast variation stability theorem.

Other parameters remain unchanged. $N_0 = 1125$ and $M = 19$ are substituted into Equation (34) to obtain the judgment result based on the fast variable stability theorem. The relationship between P and k_p when $k_i = 180$ is shown in Figure 8(a). It can be seen from the figure that when $0.20 < k_p < 1.24$, the system is in a stable state. When k_p runs outside the region [0.20, 1.24], the values of P are less than M, and the system is in a state of chaos and bifurcation, so it can be verified that the stable operating domain of k_p is [0.20, 1.24].

When $k_i = 180$, $M = 19$ and other parameters remain constant, through the analysis of fast-varying stability theorem, for the H-bridge inverter in PI control mode, when $k_i = 180$, other parameters remain unchanged. The stability region based on the fast-varying stability theorem, Figure 8 (a) is completely consistent with the bifurcation diagram of Figure 4(a) and Figure 5(a).

Similarly, for the H-bridge inverter with the joint control mode, when $k_i = 180$, the other parameters remain unchanged, and the stability region Figure 8(b) judged based on the fast-varying stability theorem is completely consistent with the analysis conclusion of the bifurcation diagram of Figure 4(b) and Figure 5(b).

V. THE INFLUENCE OF EXTERNAL CIRCUIT PARAMETERS ON THE STABILITY OF THE SYSTEM

The stability of the H-bridge inverter under the joint control mode is also related to the external circuit parameters such as input voltage-E, load inductance-L, and resistance-R.

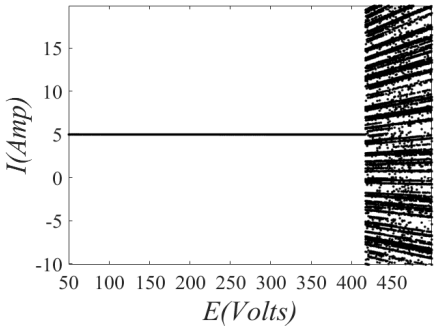

(a) bifurcation diagram of parameter E

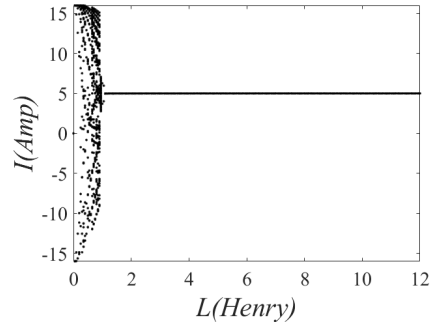

(b) bifurcation diagram of parameter L

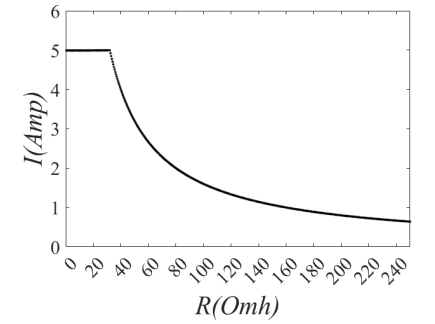

(c) bifurcation diagram of parameter R

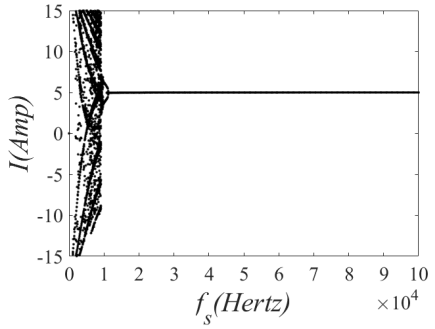

(d) bifurcation diagram of parameter f_s

FIGURE 9. Bifurcation diagrams under different circuit parameters in joint control mode.

When $k_i = 180$, the circuit parameters are as follows: $k_p = 0.6$, $f_s = 30$kHz, $i_{ref} = 5\sin(40\pi t)$, $k_1 = 0.2$, $k_2 = 0.1$, $\alpha = 0.9$. The input voltage, load inductance, load resistance and switching frequency are taken as bifurcation parameters, respectively. The bifurcation diagram of the circuit parameters varying with the external bifurcation parameters is drawn as shown in Figure 9.

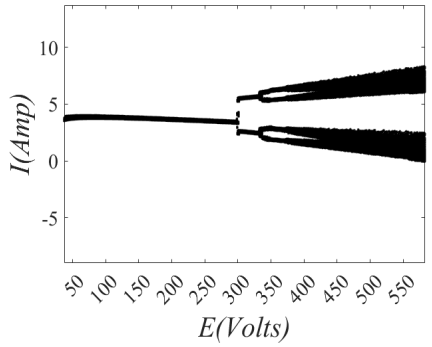

(a) bifurcation diagram of parameter E

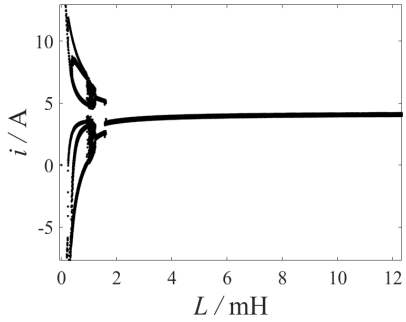

(b) bifurcation diagram of parameter L

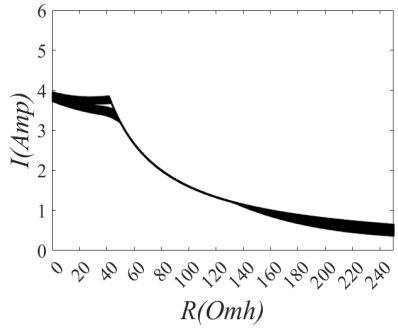

(c) bifurcation diagram of parameter R

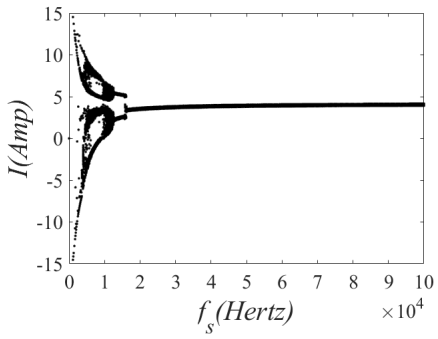

(d) bifurcation diagram of parameter f_s

FIGURE 10. Bifurcation diagrams of different circuit parameters based on PI control.

When the input voltage increases from 50V to 450V, the bifurcation diagram of the load current varies with the input voltage is drawn, as shown in Figure 9(a). In the joint control mode, the input voltage parameter is 50V∼415V and the system is in a stable state. Selected input voltage = 160V, other parameters remain unchanged, draw the bifurcation diagram

TABLE 1. Parameter stability range.

Symbol	PI Control Mode	Joint PI and improved Power reaching Law sliding Mode Control
K_p	[0.18, 1.08]	[0.20, 1.24]
E(Volts)	[50V, 295V]	[50V, 415V]
L(Henry)	[1.80mH, 12mH]	[1.15mH, 12mH]
R(Omh)	[40Ω, 120Ω]	[0Ω, 240Ω]
f_s*(Hertz)*	[17kHz, 100kHz]	[11kHz, 100kHz]

of the load inductance change, when the inductance is greater than 1.15mH, the system enters a stable state, as shown in Figure 9(b). The bifurcation diagram with the load resistance as the bifurcation parameter is drawn. As the resistance increases, the load current decreases, and the system is always in a stable state, as shown in Figure 9(c). The system reaches a steady state when the switching frequency exceeds 11 kHz, as shown in Figure 9(d) during bifurcation plotting of the change in switching frequency.

Under the same circuit parameters, draw the bifurcation diagram of input voltage, load inductance, load resistance, and switching frequency under the control of PI, as shown in Figure 10.

When the input voltage is used as the bifurcation parameter, the bifurcation diagram in the PI control mode is observed as shown in Figure 10(a), and the system stability domain is [50V,295V]. However, the stability domain of the input voltage parameter in the joint control mode is [50V,415V]. The stability domain of the H-bridge inverter system in the joint control mode is wider and more stable.

When the load inductance is used as the bifurcation parameter, as shown in Figure 10(b), the system in PI control mode starts to enter the stable state only when the inductance L increases to 1.80mH. However, in the joint control mode, the system enters the steady state when the load inductance increases to 1.15mH. The stability domain of the H-bridge inverter system in the joint control mode is wider and more stable.

When the load resistance is used as the bifurcation parameter, it is shown in Figure 10(c). The system in PI control mode enters the stable state only when the load resistance is [40Ω,120Ω]. However, the system in the joint control mode is always in a steady state when the load resistance is [0Ω,240Ω]. The stability domain of the H-bridge inverter system in the joint control mode is wider and more stable.

When the switching frequency is used as the bifurcation parameter, as shown in Figure 10(d), the system in PI control mode starts to enter the steady state only when the switching frequency is increased to 17kHz. However, in the joint control mode, the system enters the steady state when the switching frequency is increased to 11kHz. Obviously, the stability domain of the H-bridge inverter system in the joint control mode is wider and more stable.

The above numerical simulation experiments were conducted on the Matlab software platform, and the experimental results are shown in Table 1. The analysis of this parameter stability range table shows that the expansion of the system stability range in the joint control mode is reflected not only in the proportional parameter-k_p, but also in the circuit parameters. These are of great significance.

VI. CONCLUSION

The purpose of this paper is to study the nonlinear dynamic behavior of an H-bridge inverter under a joint control mode, and the stability of the system is analyzed using a bifurcation diagram, folding diagram, time-domain diagram, stroboscopic diagram, and frequency spectrum diagram. The theoretical analysis is carried out through the fast-changing stability theorem, and the conclusion of the theoretical analysis is consistent with that of numerical simulation. The stability of the system is analyzed by circuit parameters such as input voltage-E, load inductance-L, and load resistance-R. The research shows that the H-bridge inverter system under the joint control mode has a wider stability region and stronger stability. The conclusion of the study provides an important theoretical basis for the design and manufacture of an H-bridge inverter.

REFERENCES

[1] T. C. A. Ajot, S. Salimin, and R. Aziz, "Application of PI current controller in single phase inverter system connected to non linear load," *IOP Conf. Ser., Mater. Sci. Eng.*, vol. 226, Aug. 2017, Art. no. 012135, doi: 10.1088/1757-899X/226/1/012135.

[2] Y. Yu and C. Zhang, "Bifurcation analysis of cascaded H-bridge converter controlled by proportional resonant," *Int. J. Electr. Power Energy Syst.*, vol. 125, Feb. 2021, Art. no. 106476, doi: 10.1016/j.ijepes.2020.106476.

[3] H. Komurcugil, S. Biricik, S. Bayhan, and Z. Zhang, "Sliding mode control: Overview of its applications in power converters," *IEEE Ind. Electron. Mag.*, vol. 15, no. 1, pp. 40–49, Mar. 2021, doi: 10.1109/MIE.2020.2986165.

[4] L. Sun, Z. Zhou, Z. Wen, and Q. Wang, "Adaptive carrier amplitude modulation control of bifurcation and chaos in SPWM H-bridge converter," *Electr. Meas. Instrum.*, vol. 57, no. 23, pp. 101–108, 2020, doi: 10.19753/j.issn1001-1390.2020.23.014.

[5] B. Robert and C. Robert, "Border collision bifurcations in a one-dimensional piecewise smooth map for a PWM current-programmed H-bridge inverter," *Int. J. Control*, vol. 75, nos. 16–17, pp. 1356–1367, Jan. 2002, doi: 10.1080/00207170210000023771.

[6] Y. Ping, Z. Qunru, X. Zhirong, Y. Haozhe, and Z. Yuanhui, "Research on nonlinear phenomena of single-phase H-bridge inverter," in *Proc. IEEE PES Asia–Pacific Power Energy Eng. Conf. (APPEEC)*, Dec. 2014, pp. 1–6, doi: 10.1109/APPEEC.2014.7066158.

[7] L. Yang, L. Yang, F. Yang, and X. Ma, "Slow-scale and fast-scale instabilities in parallel-connected single-phase H-bridge inverters: A design-oriented study," *Int. J. Bifurcation Chaos*, vol. 30, no. 1, Jan. 2020, Art. no. 2050005, doi: 10.1142/S0218127420500054.

[8] T. Ding, Y. Zhang, P. Ju, W. Liao, and J. Fang, "Modeling H-bridge inverter based on PI control and its nonlinear dynamic behaviour," in *Proc. E3S Web Conf.* Les Ulis, France: EDP Sciences, 2022 p. 1075, doi: 10.1051/e3sconf/202236001075.

[9] S. Kasera, A. Kumar, and L. B. Prasad, "Analysis of chattering free improved sliding mode control," in *Proc. Int. Conf. Innov. Inf., Embedded Commun. Syst. (ICIIECS)*, Mar. 2017, pp. 1–6, doi: 10.1109/ICIIECS.2017.8276105.

[10] X. Hao, R. L. Xie, and X. Yang, "Research on bifurcation and chaotic behavior of first-order H-bridge inverter with sliding mode variable structure control based on pulse width modulation," *J. Phys. China*, vol. 62, no. 1, pp. 85–99, 2013, doi: 10.7498/aps.62.200503.

[11] G. Wei, W. Miao, and L. Tao, "Fractional order PID sliding mode variable structure control based inverter circuits," *Control Eng. China*, vol. 26, no. 7, pp. 1397–1404, 2019, doi: 10.14107/j.cnki.kzgc.161737.

[12] S. Maity, D. Tripathy, T. K. Bhattacharya, and S. Banerjee, "Bifurcation analysis of PWM-1 voltage-mode-controlled buck converter using the exact discrete model," *IEEE Trans. Circuits Syst. I, Reg. Papers*, vol. 54, no. 5, pp. 1120–1130, May 2007, doi: 10.1109/TCSI.2007.895526.

[13] A. A. El, M. Debbat, R. Giral, and L. Martinez Salamero, "Quasiperiodic route to chaos in DC–DC switching regulators," in *Proc. ISIE*, Pusan, South Korea, 2001, pp. 2130–2135, doi: 10.1109/ISIE.2001.932046.

[14] C. K. Tse, *Complex Behavior of Switching Power Converters*. Boca Raton, FL, USA: CRC Press, 2003, doi: 10.1201/9780203494554.

[15] H. Pan, G. Zhang, H. Ouyang, and L. Mei, "A novel global fast terminal sliding mode control scheme for second-order systems," *IEEE Access*, vol. 8, pp. 22758–22769, 2020, doi: 10.1109/ACCESS.2020.2969665.

[16] L. Liu, "Improved reaching law sliding mode control algorithm design for DC motor based on Kalman filter," *TELKOMNIKA Indonesian J. Electr. Eng.*, vol. 12, no. 12, pp. 8193–8199, Dec. 2014, doi: 10.11591/telkomnika.v12i12.4905.

[17] P. Ji, C. Li, and F. Ma, "Sliding mode control of manipulator based on improved reaching law and sliding surface," *Mathematics*, vol. 10, no. 11, p. 1935, Jun. 2022, doi: 10.3390/math10111935.

[18] X. Wang and B. Zhang, "Bifurcation and chaos analysis of single phase SPWM inverter," *Trans. China Electrotechn. Soc*, vol. 24, no. 1, pp. 101–107, 2009, doi: 10.19595/j.cnki.1000-6753.tces.2009.01.018.

[19] K. Guo, L. Zhou, and Y. Long, "The progress and trend of research on bifurcation and chaos in H-bridge converter," *J. Chongqing Univ.*, vol. 36, no. 7, pp. 52–60, 2013, doi: 10.11835/j.issn.1000-582X.2013.07.010.

[20] A. Bandyopadhyay, K. Mandal, and S. Parui, "Design-oriented dynamical analysis of single-phase H-bridge inverter," in *Proc. IEEE Int. Conf. Power Electron., Smart Grid Renew. Energy (PESGRE)*, Jan. 2020, pp. 1–6, doi: 10.1109/PESGRE45664.2020.9070760.

WEI JIANG was born in Jiangxi, China, in 1977. He received the Ph.D. degree in circuit and system from Anhui University, Hefei, China, in 2011. He is currently a Master Tutor and an Associate Professor with the Department of Intelligent Manufacturing, Wuyi University. His research interests include nonlinear circuit, nonlinear systems, and control technology.

MING JIAN WU was born in Guangdong, China. He received the bachelor's degree from Wuyi University, in 2022, where he is currently pursuing the master's degree. His research interests include nonlinear dynamic behavior and chaos control of inverter.

FANG YUAN was born in Jiangxi, China, in 1981. She received the master's degree in circuit and system from the East China University of Technology, Nanchang, China, in 2009. She is currently an Associate Professor with the Department of Electronic, East China University of Technology. Her research interests include nonlinear circuit, nonlinear systems, and test technology.